Vertically Aligned Nanopillar Arrays with Hard Skins Using Anodic Aluminum Oxide for Nano Imprint Lithography

Pyung-Soo Lee, Ok-Joo Lee, Sun-Kyu Hwang, Seung-Ho Jung, Sang Eun Jee, and Kun-Hong Lee*

Department of Chemical Engineering, Computer & Electrical Engineering Division, Pohang University of Science and Technology (POSTECH), Pohang 790-784, Korea

Received August 17, 2005. Revised Manuscript Received September 25, 2005

Master molds with nano-pillar structures were fabricated by using anodic aluminum oxide (AAO) for nano-imprint lithography (NIL). The proposed method consists of (1) AAO fabrication, (2) transfer of the thin AAO layer onto a substrate, (3) aluminum sputtering, (4) aluminum melting, and (5) removal of the thin AAO layer. Since the sputtered aluminum penetrated into the porous alumina walls of the AAO template during the melting step, the pillars had skin layers of aluminum/alumina composite which added additional mechanical strength and chemical resistance. The diameter of a pillar in the nano-pillar master mold was larger than that of the hole diameter of the original AAO template because of the hard skin of aluminum/alumina composite layer which covers the pillar surface. The pillar structure could be used as a mold for NIL, resulting in a regular pore array on a polymer film.

Introduction

Regular patterns at the nanometer scale are omnipresent in nature. They also play a central role in artificial systems such as semiconductors, flat panel displays, photonic crystals, and nano-electromechanical systems (NEMS).[1−3] The performances of these nano-devices depend heavily upon the resolution and versatility of patterning techniques.[4]

Photolithography has been the standard technique for the fabrication of microscopic patterns in semiconductor industries due to its versatility and high throughput. The technique, however, becomes impractical, both technically and economically, at feature sizes smaller than the wavelength of the applicable light. Next generation lithography techniques, such as extreme UV lithography (EUVL) or X-ray lithography, still require much effort before they can be fully implemented as commercial production methods.[5,6]

Novel patterning methods which have been investigated to fulfill the need for nanoscale patterning include e-beam lithography,[7] dip-den lithography,[8] nano-imprint lithography (NIL),[9] microcontact printing,[10] self-assembly monolayer,[11] just to name a few. None have yet shown the full potential to be the next generation fabrication method with high versatility and throughput.

NIL has recently been advanced greatly and has become a strong candidate for the next generation fabrication technique for nano-patterns.[12] Parallel replication of nano-patterns down to a resolution of a few nanometers can be obtained in a single step, simply by pressing the mold having nano-structures onto the polymer layer. The mold should endure a pressure above 1MN during NIL. Additional requirements for the mold include chemical resistance, weak adhesion to polymers, and the mechanical strength to avoid distortion and breakage during peeling off. These requirements make hard materials such as SiO_2, SiC, and diamond the best choice for mold materials.[13−15] Although NIL has a great potential as a high throughput fabrication technique, the mold itself should be fabricated through time-consuming e-beam lithography and dry etching when these hard materials are used as molds.

Anodic aluminum oxide (AAO) is formed through anodic oxidation of pure aluminum. AAO has parallel pores of tens of nanometers wide, separated by regular distances, and is easily scalable to a large area. Nanotubes and nanowires have been synthesized by filling these pores with organic as well as inorganic materials.[16,17] Molds with parallel pillars have

* Corresponding author. Fax: +82-54-279-8298. E-mail: ce20047@postech.ac.kr.

(1) Moreau, W. M. *Semiconductor Lithography-Principles and Materials*; Plenum: New York, 1998.
(2) Joannopoulos, D. J.; Meade, D. R.; Winn, N. W. *Photonic Crystals-Molding the Flow of Light*; Princeton University Press: Princeton, NJ, 1995.
(3) Sergey, E. L. *Nano- and Micro- Electromechanical Systems-Fundamentals of Nano- and* Microengineering; CRC press: New York, 2000.
(4) Marrian, C. R. K.; Tennant, D. M. *J. Vac. Sci. Technol. A* **2003**, *21* (5), S207.
(5) Geppert, L. *IEEE Spectrum* **1996**, *33* (4), 33.
(6) Prease, R. F. W. *J. Vac. Sci. Technol. B* **1992**, *10* (1), 278.
(7) Bard, A. J.; Denault, G.; Lee, C.; Mandler, D.; Wipf, D. O. *Acc. Chem. Res.* **1990**, *23*, 357.
(8) Richard, D. P.; Zhu, J.; Xu, F.; Hong, S. J. *Science* **1999**, *283*, 661.
(9) Chou, S. Y.; Krauss, P. R.; Renstorm, P. J. *Science* **1996**, *272*, 85.
(10) Kumar, A.; Whitesides, G. H. *Appl. Phys. Lett.* **1993**, *63*, 2002.
(11) Kumar, A.; Licholals, L. A.; Abbott; Kim, E.; Hans, A. B.; Whitesides, G. M. *Acc. Chem. Res.* **1995**, *28*, 219.
(12) Guo, L. J. *J. Phys. D: Appl. Phys.* **2004**, *37*, R123.
(13) Chou, S. Y.; Krauss, P. R.; Zhang, W.; Guo, L.; Zhuang, L. *J. Vac. Sci. Technol. B* **1997**, *15* (6), 2897.
(14) Pang, S. W.; Tamamura, T.; Nakao, M.; Ozawa, A.; Masuda, H. *J. Vac. Sci. Technol. B* **1998**, *16* (3), 1145.
(15) Taniguchi, J.; Tokano, Y.; Miyamoto, I.; Komuro, M.; Hiroshima, H. *Nanotechnology* **2002**, *13*, 592.
(16) Jeong, S. H.; Lee, O. J.; Lee, K. H.; Oh, S. H.; Park C. G. *Chem. Mater.* **2002**, *14* (10), 4003.
(17) Hwang, S. K.; Jeong S. H.; Lee O. J.; Lee, K. H. *Microelectron. Eng.* **2005**, *77*, 2.

10.1021/cm051855j CCC: $30.25
Published on Web 10/29/2005

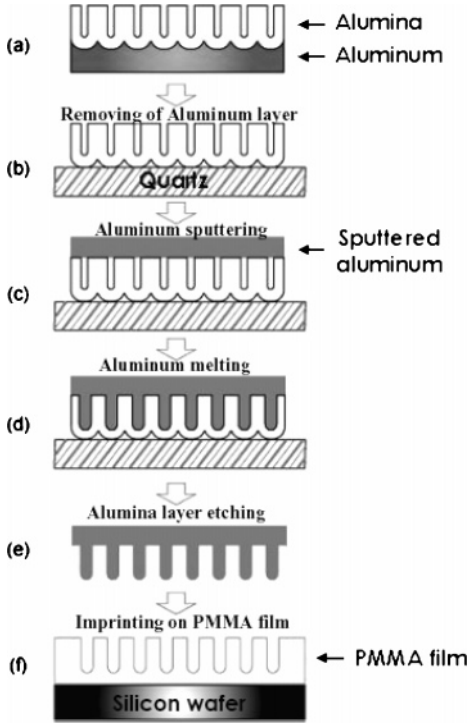

Figure 1. Overall fabrication process. (a) Fabrication of an AAO template by using two-step anodization. (b) Removal of the underlying aluminum layer and attachment of the AAO template on a quartz plate. (c) Sputter deposition of thin aluminum layer on top of the AAO template. (d) Filling of the pores with molten aluminum by heating. (e) Removal of the AAO template by wet-etching. (f) Fabrication of the polymer film with nanoholes by NIL.

also been reported with Poly(methyl methacrylate), copper, and carbon.[18−20] Although the fabrication process of these pillar structures is straightforward, the pillars are either not strong enough mechanically or chemically or poor in dimensional precision. As a result, vertically aligned pillar structures applicable as a NIL mold have not yet been reported.

In this work, we propose a fabrication method of NIL molds using AAO as a starting material. The proposed method consists of (1) AAO fabrication, (2) transfer of the thin AAO layer onto a substrate, (3) aluminum sputtering, (4) aluminum melting, and (5) removal of the thin AAO layer. Since the sputtered aluminum penetrates the porous alumina walls during the melting step, the pillars have skin layers of aluminum/alumina composite which add additional mechanical strength and chemical resistance. The pillar structure could be used as a mold for NIL, resulting in a regular pore array on a polymer film.

Experimental Section

The fabrication sequence of the master mold is shown in Figure 1. An AAO template was prepared by the electropolishing and two-step anodization of pure aluminum sheets (99.999%, Good Fellow). First, the specimen was electropolished in a mixture of perchloric acid and ethanol ($HClO_4$:C_2H_5OH = 1:4 in volumetric ratio) at 7 °C for 3 min to remove surface irregularities. Anodization was then carried out with 0.1 M phosphoric acid (85%, Aldrich) at 195 V and 0 °C for 16 h. After the first anodization, the porous alumina layer was etched away by alumina etchant (1.8 wt % chromic acid and 6 wt % phosphoric acid) at 65 °C for 5 h, and the second anodization was performed at the identical conditions as the first anodization, but only for 5 min (Figure 1a)]. The AAO template was separated from the underlying aluminum substrate by etching with a saturated mercuric chloride (99.5%, Samchun Chemical) solution at 20 °C for 30 min, and then it was mounted on a quartz plate (Figure 1b). Next, a pure aluminum layer of 3 μm thickness was deposited using a DC Ar plasma onto the AAO template at 0.22 A, 350 V, and 2×10^{-2} Torr (Figure 1c). The aluminum was then melted at 700 °C and 1 atm Ar atmosphere for 2 h to fill the pores of the template (Figure 1d). Removal of the AAO template with the same alumina etchant completed the fabrication process of the master mold having parallel pillar structures (Figure 1e). Finally, a NIL process was carried out to test the capability of the master mold. To test the hardness of the pillar structure, it was pressed on a smooth aluminum sheet with a 3 MPa pressure. Next, a poly(methyl methacrylate) (PMMA, Mw 11000, polymer standard) film of 100 nm thickness was prepared on a Si wafer by spin-coating a solution of 4.0 wt % PMMA in toluene. The PMMA film was preheated to 90 °C for 5 min, and then the master mold was pressed onto the PMMA film at 1.5 MPa for 5 min using a hot press (ISTC). The master mold was separated from the PMMA film after the temperature was cooled to below 40 °C. Figure 1f represents the air pillar structures in the PMMA film. The morphology of the sample in each step was observed by using a field emission-scanning electron microscope (FE-SEM, PHILIPS XL 30S FEG). An ellipsometer (EC-400, J. A. Woollan Co. Inc.) was used to measure the refractive indices of the PMMA film with air pillars.

Results and Discussion

AAO templates were fabricated by a two-step anodization in phosphoric acid. A long anodization of 16 h was necessary to obtain a well-arranged pore array. Figure 2a shows the current density vs anodization time characteristics. Three distinctive regions exist in this figure. A high current density, over 1 A cm^{-2}, was initially applied at a constant voltage of 195 V to form the oxide layer on the surface of the aluminum sheet. The current density abruptly decreased to 1 mA cm^{-2}, and the color of the specimen changed to bright purple. This low current density was maintained for 30 min without any change in the color of the specimen (region 1). Later, the current density gradually increased, and the color of the specimen changed to dark gray (region 2). Random pores start developing in this transition period, and the diameters grow until reaching a steady state at the current density of about 8 mA cm^{-2}, and it remained until the first anodization ended (region 3). Figure 2b shows the cross section of the specimen after the first anodization. The uppermost part of the AAO shows pores with different diameters and imperfect pore arrangement. However, as anodization proceeds (going lower in the specimen), regularity in pore arrangement greatly improves, and the straight pore array and ordered cell configuration were obtained.

Next, the AAO was completely etched away, and the perfectly ordered concave patterns on the surface of the aluminum specimen were excavated. Then, the second anodization was carried out at identical conditions. Figure 3 shows SEM images of the AAO after the second anodization.

(18) Masuda, H.; Fukuda, K. *Science* **1995**, *268*, 1466.
(19) Shingubara, S.; Okino, O.; Sayama, Y.; Sakaue, H.; Takahagi, T. *Solid-State Electron.* **1999**, *43*, 1143.
(20) Rahman, S.; Yang, H. *Nano Lett.* **2003**, *3* (4), 439.

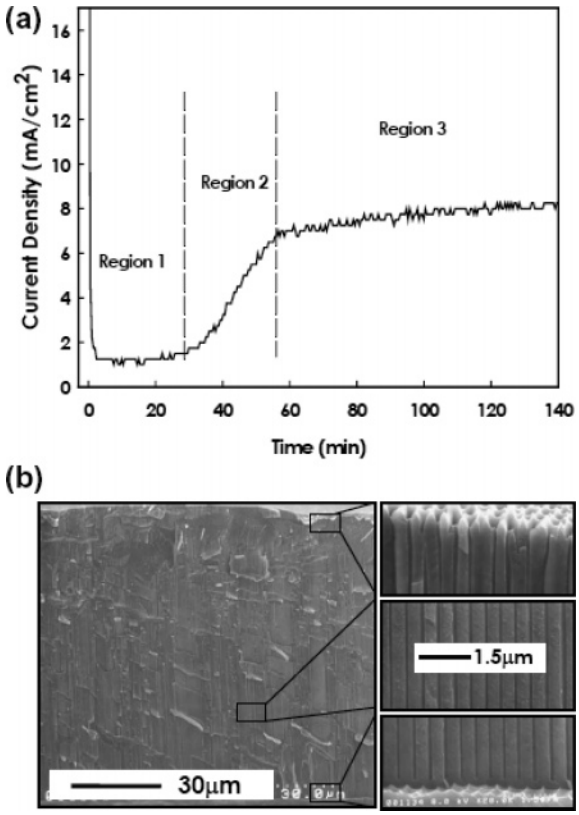

Figure 2. (a) Change of the current density during first anodization. (b) Cross section of the aluminum specimen after first anodization.

A perfect array of pores with a hexagonal configuration is observed in Figure 3a. The pore diameter and the interpore distance are 100 and 500 nm, respectively. The cross-sectional view of the sample in Figure 3b discloses that the shape of the pore is, in fact, similar to a funnel. The second anodization was carried out for 5 min to obtain this 800 nm thick sample.

Nano-pillar structures were fabricated by filling aluminum into the pores of the AAO template. The specimen after anodization consists of two parts: the upper AAO layer and the lower aluminum substrate. The AAO layer was separated from the underlying aluminum substrate by wet-etching. This was necessary because the melting point of aluminum is only 665 °C, and we have to fill molten aluminum into the pores of the AAO template to make a mold. The AAO template is only 800 nm thick, flexible, and apt to roll. Therefore, the AAO template was mounted on a quartz plate for easy handling. The quartz plate and the AAO template were well bound together because of the large surface energy of the thin AAO template.

Alumina undergoes a phase transition, amorphous to gamma alumina, in the range of 820−840 °C with the generation of micropores and cracks.[21] Therefore, the filling material should have a lower melting point than this temperature. At the same time, the filling material should have a high strength after solidification to be used as a mold. Aluminum certainly meets the first requirement, but it is so soft, compared to other NIL mold materials such as Si and SiO_2, that it is apt to be damaged during the NIL process.[13−15]

(21) Mardilovich, P. P.; Govyadinov, A. N.; Mukhurov, N. I.; Rzhevskii, A. M.; Paterson, R. *J. Membr. Sci.* **1995**, *98*, 131.

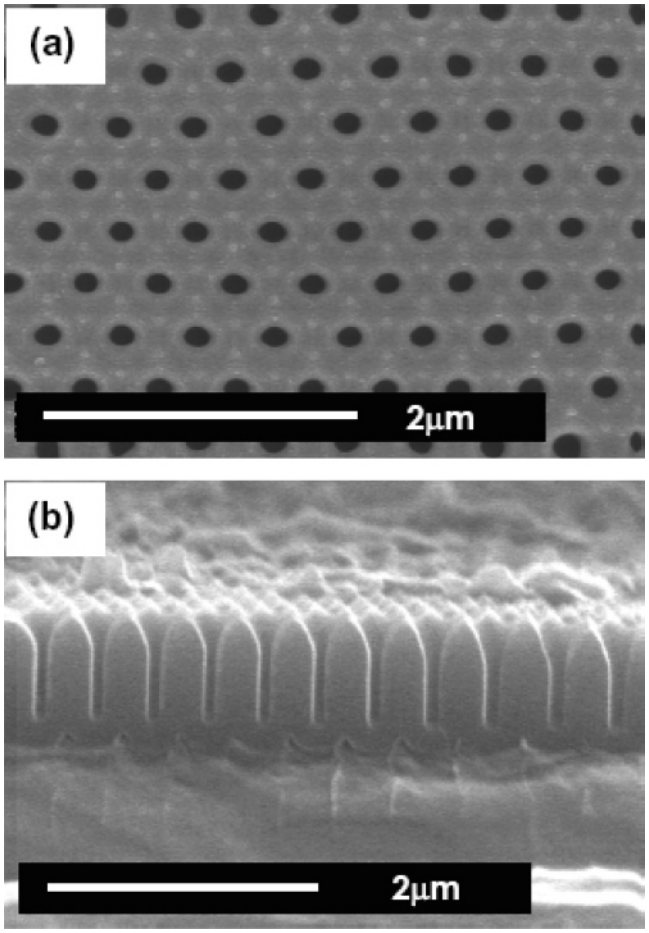

Figure 3. Morphology of the AAO template after second anodization. (a) Top view. (b) Cross-sectional view.

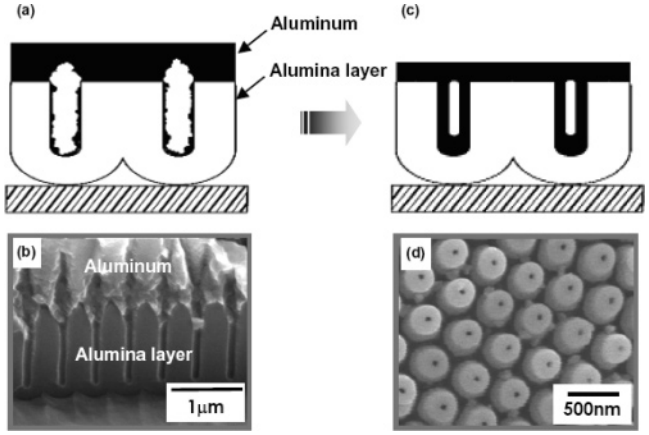

Figure 4. Nano-pillar formation by melting. (a) AAO template after aluminum sputtering (schematic). (b) AAO template after aluminum sputtering (cross-sectional view). (c) Hole filling with molten aluminum. (d) Hollow nano-pillars (after Ar milling). Ar milling was performed at 5×10^{-4} Torr for 1 h with a 80W power. The sample was held at a 45° angle to the ion source.

In fact, most of the metals having melting point below 1000 °C show poor hardness. Fortunately, the pore walls of an AAO template contain many tiny holes, and molten aluminum penetrates these holes,[22] resulting in an aluminum/alumina skin with a higher hardness.[23,24] We were able to make the aluminum molds with hard skins by taking advantage of this phenomenon.

Figure 4 represents the mechanism of the formation of aluminum pillars by filling of molten aluminum into the pores

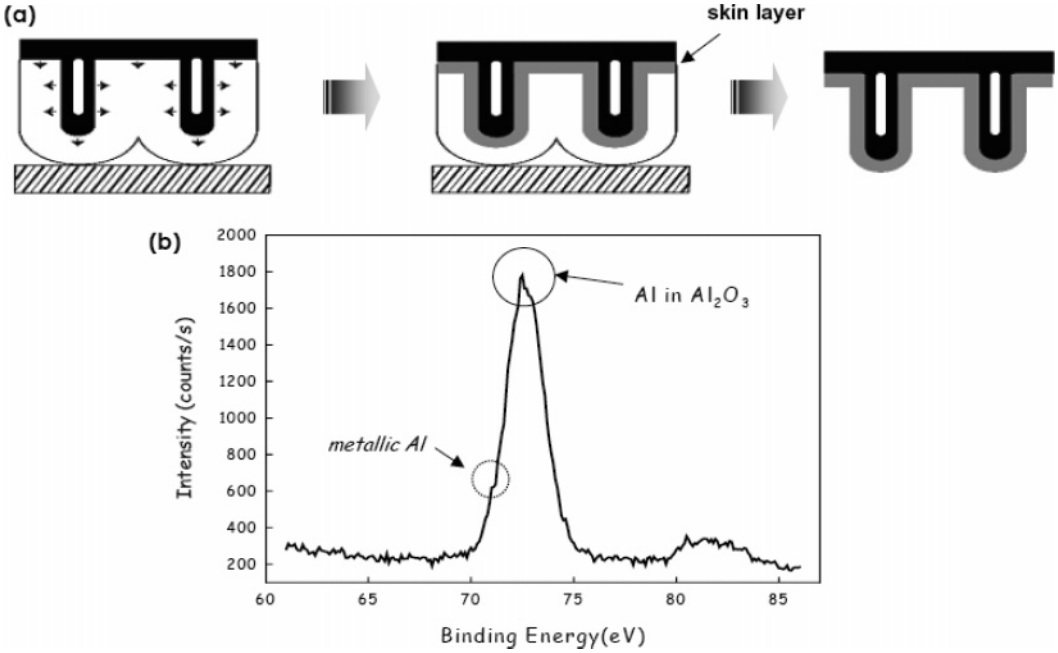

Figure 5. Alumina/aluminum skin layer. (a) Fabrication process of nano-pillars (schematic). (b) Atomic analysis of the nano-pillars. XPS analysis was carried out with an EscaLab 220-IXL using un-monochromatized incident Mg X-ray radiation.

of an AAO template. Aluminum is deposited on the surface of an AAO template as well as inside the pores of the AAO template. The pores are closed by the sputtered aluminum much faster than they are filled due to their high aspect ratio of the pores (Figure 4a). Therefore, sputtering alone generates large voids inside the pores (Figure 4b), so the melting step should follow to obtain metal pillars. Frequently, incomplete filling of the pores by molten aluminum occurs, resulting in hollow cylindrical pillars (Figure 4c). To confirm these hollow pillar structures, the AAO template was separated from the quartz plate, and Ar milling and alumina etching were carried out on the bottom part of the AAO template. (The etching process will be explained later in detail.) Small holes were observed at the center of each pillar, as we had expected (Figure 4d).

After aluminum melting, the specimen in Figure 4c was selectively etched in alumina etchant in order to remove the AAO template and obtain the nano-pillar mold. The alumina etching solution is a mixture of phosphoric acid and chromic acid. Phosphoric acid is a corrosive material and dissolves alumina and aluminum. On the other hand, chromic acid protects aluminum from the corrosive acid by forming an oxide cover on the surface.[25] Therefore, the alumina etchant could only dissolve the alumina layer since the aluminum was protected, resulting in the aluminum nano-pillar mold.

Figure 5a shows a schematic of the formation of the alumina/aluminum composite layer on the surface of nano-pillars. Molten aluminum not only fills the pores of the AAO template but also penetrates the porous pore walls during the melting process, forming the penetration layer of alumina/aluminum composite.[22] This composite layer has many desirable properties such as corrosion resistance as well as fracture toughness and enhances bending strength and hardness.[23,24]

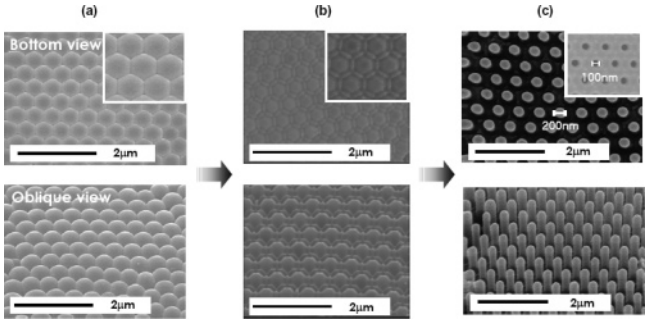

Figure 6. Change of morphology during etching. (a) Hexagonally arranged hemispherical cells. (b) Overlapping of cells during etching. (c) Nano-pillar structures after complete etching.

X-ray photoelectron spectroscopy analysis (XPS) of the nano-pillar mold shows the Al 2p metallic peak at 72 eV, but only as a small shoulder with the dominant Al 2p oxide peak. The etching of the alumina/aluminum composite layer (gray region) took much longer than that of the porous alumina layer (white region), so a more prominent metallic peak was expected. This inconsistency partly comes from the small concentration of aluminum in the composite layer. In-depth analysis of the composite layer is ongoing.

Figure 6 shows the change of morphology during the etching process. These SEM images are the bottom views of the sample in Figure 5. Ordered hexagonal cells were initially observed (Figure 6a). The oblique view reveals that these hexagonal cells actually have a hemispherical shape. As the etching proceeds, the ordered hexagonal cells appear to overlap (Figure 6b). This is because the etching rate of the boundary region between two cells is much slower than that of the inner part of a hexagonal cell. Therefore, the

(22) Garcia-Mendez, M.; Valles-Villarreal, N.; Hirata-Flores, G. A.; Farias, H. M. *Appl. Surf. Sci.* **1999**, *151*, 139.
(23) Moon, R.; Tilbrook, M.; Hoffman, M. J.; Neubrand, A. *J. Am. Ceram. Soc.* **2005**, *88* (3), 666.
(24) Mattern, A.; Huchler, B.; Staudenecker, D.; Oberacker, R.; Nagel, A.; Hoffman, M. J. *J. Eur. Ceram. Soc.* **2004**, *24* (12), 3399.
(25) Jones, D. A. *Principles and Prevention of Corrosion*; Macmillan Pub. Co.: New York, 1996.

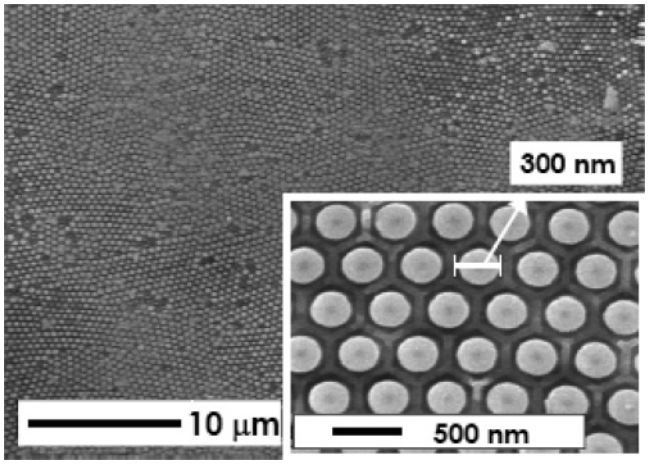

Figure 7. Large-scale master mold.

boundaries gradually become more protruded,[26] and the nano-pillar structure was finally obtained when the alumina layer was completely etched (Figure 6c). This specific sample contains vertically aligned pillars with a 200 nm diameter. Interestingly, the diameter of a pillar is twice that of the hole diameter of the original AAO template. Therefore, this nano-pillar has a 50 nm thick hard skin of aluminum/alumina composite layer.

The diameter of the nano-pillars can be freely controlled either by starting with AAO templates having different hole diameters or by changing aluminum melting times. A combination of the two methods is equally possible. As a demonstration, an AAO template having 150 nm diameter holes was used to fabricate nano-pillars under the same conditions in Figure 6c except for a 2.5 h aluminum melting time. The nano-pillar structure thus fabricated has a 300 nm pillar diameter (Figure 7). These nano-pillars have a 75 nm thick hard skin.

The pillar structure was successfully formed throughout a large area, though roughly 10% of the pillars was imperfect. Note that hexagonal walls appear at the boundaries of each pillar as in the inset of Figure 7. The alumina layer (the white region in Figure 5) of an AAO template is actually composed of two sub-regions: an acid-contaminated region and an almost pure alumina region. Since the etching rate of the acid-contaminated region is much faster than that of the pure alumina region,[26] these hexagonal walls appear during etching.

The hardness of nano-pillars is greatly improved by the presence of the aluminum/alumina composite layer on the surface of nano-pillars. Figure 8a shows the surface morphology of the aluminum plate after pressing with the nano-pillar structure. Here, nano-holes (or indents) are clearly seen. If the nano-pillars were no harder than pure aluminum, the nano-pillars might be broken or squashed during pressing, and the ordered nano-hole structure could not be formed on the aluminum plate. Due to the hard skin layer, the nano-pillar structure had enough hardness to indent aluminum.

To obtain our final goal, the NIL process was carried out using the nano-pillar structure as a master mold. Because of the hard skin on the nano-pillar structure and the vertically aligned pillars, ordered polymer holes were successfully patterned on a polymer surface (Figure 8b). The polymer structure was an exact replica of the AAO template except for the hole diameter. Moreover, although an antiadhesion layer was not used between the master mold and the polymer substrate during the NIL process, they were easily separated.

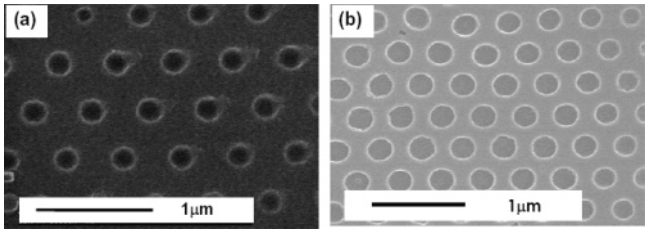

Figure 8. Nano-holes formed through the NIL process. (a) Aluminum plate. (b) PMMA film.

The refractive index depends highly on the porosity of the material when the scale of the pores is smaller than the wavelength of light.[27] Since the dimension of the pillars in the nano-pillar structure can be controlled, porosity (and thus the refractive index) of a thin polymer film can also be controlled by using this nano-pillar mold. To prove this concept, the refractive index of polymer films was measured by an ellipsometer. The refractive index of PMMA having a smooth surface was 1.49, but that of the polymer film with nano-holes decreased to 1.40. The PMMA film has 20% of porosity due to the nano-holes in it, and this porosity contributes to the decrease in the refractive index. Further investigation is ongoing.

Conclusion

The fabrication method proposed in this work gives an alternative route to the fabrication of NIL master molds without resorting to conventional lithography. Aluminum penetrates the porous alumina walls of an AAO template at high temperatures, and we took advantage of this phenomenon to make a nano-pillar structure. This structure has high resistance to the corrosive etching solution as well as good hardness due to the aluminum/alumina composite skin thus formed. Using this nano-pillar structure as a master mold, we have successfully obtained a polymer substrate with hexagonally arranged nano-holes through the NIL process. The reduction of the refractive index of this polymer film suggests the possibility of application in optics requiring a low reflective index such as antireflection films. The demonstrated method has the merits of cost-effectiveness and easy scalability to a large area.

Acknowledgment. The authors would like to thank the Ministry of Education of Korea for its financial support of the Electrical and Computer Engineering Division at POSTECH through the Brain Korea 21 (BK21) program. This work is also supported by the National R&D Project for Nano Science and Technology.

CM051855J

(26) Mardilovich, P. P.; Alexander, N. G.; Nadezhda, I. M.; Raterson, R. *J. Membr. Sci.* **1995**, *98*, 143.

(27) Macleod, H. A. *Thin-film Optical Filters*; Macmillan Pub. Co.: New York, 1986.